Electrocoagulation Studies on the Removal of Copper from Water Using Mild Steel Electrode

Subramanyan Vasudevan[1]*, Jothinathan Lakshmi[2], Ganapathy Sozhan[3]

ABSTRACT: This study provides an electrocoagulation process for the removal of copper from water using mild steel and stainless steel as anode and cathode, respectively. The effect of different operating parameters and coexisting ions on the removal efficiency of copper was investigated. The results showed that the optimum removal efficiency of 97.8% was achieved at a current density of 0.02 A/dm^2 and a pH of 7.0. The adsorption of copper, preferably fitting the Langmuir adsorption isotherm, suggests monolayer coverage of adsorbed molecules. First- and second-order rate equations and Elovich and intraparticle diffusion models were applied to study adsorption kinetics. The adsorption process follows the second-order kinetics model with good correlation. Temperature studies showed that adsorption was endothermic and spontaneous in nature. *Water Environ. Res.*, **84,** 209 (2012).

KEYWORDS: copper removal, electrocoagulation, adsorption kinetics, isotherms.

doi:10.2175/106143011X13225991083640

Introduction

The presence of heavy metals in an aquatic environment is cause for great environmental concern. Copper, which is one of the most toxic heavy metals to living organisms, is one of the more widespread heavy metal contaminants in the environment (James et al., 2006; Vinikour et al., 1980). Copper, a metal that occurs naturally in rocks, soil, water, and air, is an essential element in plants, animals, and humans (Billon et al., 2006). The adverse health effects caused by copper, mercury, and arsenic poisoning are far more catastrophic than any other natural calamity in the world in recent times (Onmez and Aksu, 1999; Ozer et al., 2004; Papandreou et al., 2007; Prasad and Freitas, 2000). Potential sources of copper in industrial effluents include metal cleaning and plating baths, pulp, paperboard mills, wood pulp production, the fertilizer industry, paints and pigments, municipal and stormwater runoff, and so on (Boujelben et al., 2009). Common symptoms of copper toxicity are injury to red blood cells and lungs; copper toxicity can also damage liver and pancreatic functions. Long-term exposure to copper may cause irritation to the nose, mouth, and eyes, and also may cause headaches, stomachaches, dizziness, vomiting, and diarrhea (Ajmal et al., 1998; Bailey et al., 1999; Gardea-Torresdey et al., 1996; Ozcan et al., 2005; Yu et al., 2000). As recommended by the World Health Organization, the drinking water guideline value for copper is 2 mg/L. The U.S. Environmental Protection Agency has set the maximum contaminant level allowable in drinking water for copper at 1.3 mg/L (CPCB, http://www.cpcb.nic.in). Conventional methods for removing copper from water include ion exchange, reverse osmosis, coprecipitation, coagulation, electrodialysis, and adsorption (Fiol et al., 2006; Ozcan et al., 2005; Saeed et al., 2005; Shukla and Sakhardane, 1992; Villaescesa et al., 2004). Physical methods such as ion exchange, reverse osmosis, and electrodialysis have proven to be either too expensive or inefficient to remove copper from water. Presently, chemical treatment methods are not being used because of heavy maintenance costs, problems pertaining to sludge handling and its disposal, and neutralization of effluent. Recent studies have demonstrated that the electrocoagulation method offers an attractive alternative to traditional methods for treating water. In this process, anodic dissolution of metal electrode takes place with the evolution of hydrogen gas at the cathode. Electrochemically generated metallic ions from the anode can undergo hydrolysis to produce a series of activated intermediates that are able to destabilize finely dispersed particles present in the water to be treated. The advantages of electrocoagulation are high particulate removal efficiency, compact treatment facility, and the possibility of complete automation (Vasudevan et al., 2009; 2010). This method is characterized by reduced sludge production, a minimum requirement of chemicals, and ease of operation (Adhoum and Monser, 2004; Bailey et al., 1999; Carlesi Jara et al., 2007; Carlos et al., 2006; Chen, 2004; Christensen et al., 2006; Mrozowski and Zielinski, 1983; Miwa et al., 2006; Onder et al., 2007; Vasudevan et al., 2009; 2010). The overall reactions for iron and aluminium are as follows:

$$\text{Iron electrode: } 4Fe(aq) + 10H_2O + O_2 \rightarrow 4Fe(OH)_3 + 10H_2 \quad (1)$$

$$\text{Aluminium electrode: } Al^{3+}(aq) + 3H_2O \rightarrow Al(OH)_3 + 3H^+(aq) \quad (2)$$

Although there are numerous reports on electrochemical coagulation as a means of removal of many pollutants from water and wastewater, there are few studies on copper removal by the electrocoagulation method. In this study, mild steel has been used as anode and stainless steel as cathode for removal of copper from water through the electrocoagulation process. To optimize the maximum removal efficiency of copper, the different parameters such as effect of initial concentration, effect of temperature, effect of current density, and effect of pH were studied. In doing so, the equilibrium adsorption behavior is analyzed by fitting models of Langmuir, Freundlich, and Dubinin–Redushkevich isotherms. Adsorption kinetics of electrocoagulants are analyzed using first- and second-order, Elovich, and intraparticle kinetic models. The activation energy is evaluated to study the nature of adsorption.

[1]* [2, 3] Central Electrochemical Research Institute, Karaikudi 630 006, India; e-mail: vasudevan65@gmail.com.

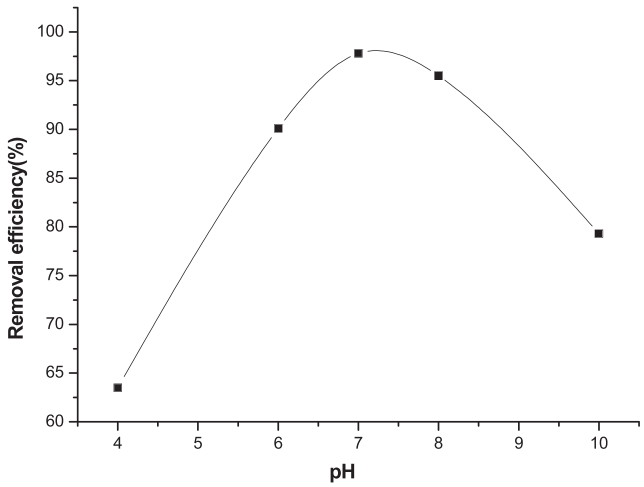

Figure 1—Effect of pH on the removal of copper at a current density of 0.02 A/dm^2, concentration 10 mg/L, and temperature of 303 K.

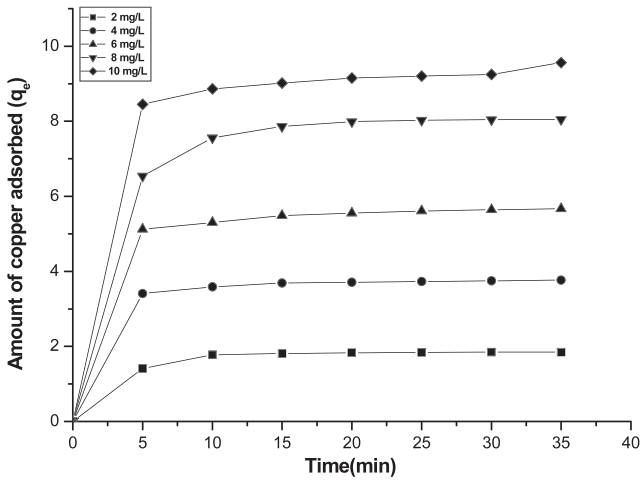

Figure 2—Effect of electrolysis time and amount of copper adsorbed at a current density of 0.02 A/dm^2, pH 7.0, and a temperature of 303 K.

Materials and Methods

Experimental Apparatus and Procedures. The electrochemical cell consists of a 1.0-L glass vessel fitted with a polyvinyl chloride (PVC) cover having suitable holes to introduce the electrodes, thermometer, pH sensor, and electrolyte. Mild steel sheet (Alfa Aesar; size 2 dm^2) was used as anode and stainless steel was used as cathode. The inter electrode gap between anode and cathode was 0.5 cm. The temperature of the electrolyte was controlled to the desired value with variation of $\pm$ 2 K by adjusting the rate of flow of thermostatically controlled water through an external glass-cooling spiral. A regulated direct current was supplied from a rectifier (10 A, 0 to 25 V; Aplab model).

Copper nitrate $Cu(NO_3)_2$ (Analar reagent) was dissolved in deionized water for the required concentration (2 to 10 mg/L). The pH of the electrolyte was adjusted, if required, with 1-M HCl or NaOH solutions. Temperature studies were carried out at varying temperatures (313 to 343 K) to determine the type of reaction. To examine the effect of coexisting ions on the removal of copper, Analar-grade sodium salts of carbonate (0 to 250 mg/L), phosphate (0 to 50 mg/L), silicate (0 to 15 mg/L), and fluoride (0 to 5 mg/L) were added to the electrolyte in required concentrations.

For scale-up studies, a volume of 7.5 L was used for each experiment as the electrolyte and electrolysis were carried out at a flowrate of 2 L/hr. A tank (0.40 [length] $\times$ 0.35 [width] $\times$ 0.35 m [height]) was fitted with PVC cover with suitable holes to fix the anode, cathode, thermometer, and electrolyte, which acted as the cell. Mild steel and stainless steel sheets of 0.17 (width) $\times$ 0.18 m (height) were used as the anode and cathode, respectively. The cell was operated at a current density of 0.02 A/dm^2, a concentration of 10 mg/L, a temperature of 305 K, and an electrolyte pH of 7.0.

Analytical Procedure. Copper was analyzed using a UV-visible spectrophotometer (Spectroquant Pharo 300; MERCK, Darmstadt, Germany). The scanning electron microscope (SEM) and energy-dispersive X-ray spectroscopy of copper-adsorbed iron hydroxide coagulants were analyzed with an SEM made by Hitachi (model s-3000h; Hitachi Ltd., Tokyo, Japan). The X-ray diffraction of electrocoagulation byproducts was analyzed by a JEOL X-ray diffractometer (JEOL Ltd., Tokyo, Japan). The Fourier transform infrared (FTIR) spectrum of iron hydroxide was obtained using Nexus 670 FTIR spectrometer (Thermo Electron Corporation, Waltham, Massachusetts). Concentrations of carbonate, silicate, fluoride, and phosphate were determined using a UV-visible spectrophotometer (Spectroquant Pharo 300, MERCK).

Results and Discussion

Effect of Electrolyte pH. Initial pH of the electrolyte is an important factor affecting the performance of electrochemical processes, particularly the performance of electrocoagulation. To evaluate its effect, a series of experiments were performed using 10 mg/L of copper-containing solutions, with an initial pH varying in the range of 4 to 10. Figure 1 shows that copper removal efficiencies increased with increasing pH and highest removal efficiencies were obtained at pH 7.0. In the case of iron anode, when solution pH becomes acidic, the oxidation of ferrous iron (Fe II) to ferric iron (Fe III) diminishes and, therefore, copper removal efficiency decreases. Neutral and slightly alkaline pH, however, tends to favor Fe (II) to Fe (III) oxidation and complex polymerization. Finally, hydroxylated colloidal polymers and an insoluble precipitate of hydrated ferric oxide were formed and removal efficiency was increased.

Effect of Initial Copper Concentration. To study the effect of initial concentration, experiments were conducted at varying initial concentrations from 2 to 10 mg/L; the results are illustrated in Figure 2. The results show that the adsorption of copper is increased with an increase in copper concentration and that it remains constant after equilibrium time. The equilibrium time was 10 minutes for all of the concentrations studied (2 to 10 mg/L). The amount of copper adsorbed at equilibrium (q_e) increased from 1.81 to 8.65 mg/g when the concentration was increased from 2 to 10 mg/L. The figure also shows that the adsorption was rapid during the initial stages and gradually decreased with the progress of adsorption. The plots are single, smooth and continuous curves leading to saturation, suggesting the possible monolayer coverage to copper on the surface of the adsorbent (Ozcan et al., 2005; Vasudevan et al., 2009; 2010).

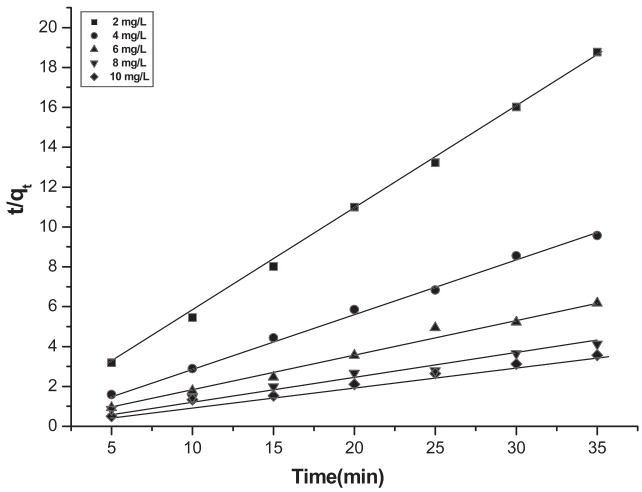

Figure 3—Second-order kinetic model plot of different concentrations of copper at a current density of 0.02 A/dm^2, temperature of 303 K, and pH 7.0.

Effect of Current Density. Among the various operating variables, current density is an important factor that strongly influences the performance of electrocoagulation. To investigate the effect of current density, a series of experiments were carried out using 10 mg/L of copper-containing electrolyte at a pH 7.0, with the current density varied from 0.01 to 0.125 A/dm^2. The removal efficiencies of copper are 95, 97.8, 98.1, 98.3, 98.7, and 99.1% for current densities 0.01, 0.02, 0.5, 0.75, 0.1, and 0.125 A/dm^2, respectively. It was found that, beyond 0.02 A/dm^2, the removal efficiency remains almost constant at higher current densities. Hence, further studies were carried out at 0.02 A/dm^2. The results showed that the removal of copper increases with increases in current density. This can be attributed to an increase in the amount of iron hydroxide being generated in situ, thereby resulting in rapid removal of copper (Vasudevan et al., 2009; 2010). The amount (i.e., average value) of adsorbent [Fe$(OH)_3$] was determined from the Faraday law, as follows:

$$E_c = ItM/ZF \quad (3)$$

Where

I = current in A,
t = the time s,
M = the molecular weight,
Z = the electron involved, and
F = the Faraday constant (96485.3 coulomb mole^{-1}).

As expected, the amount of copper adsorption increases with the increase in adsorbent concentration, which indicates that the adsorption depends on the availability of binding sites for copper.

Effect of Coexisting Ions. *Carbonate.* The effect of carbonate on copper removal was evaluated by increasing the carbonate concentration from 0 to 250 mg/L in the electrolyte. The removal efficiencies are 97.8, 97, 79, 67.2, 33, and 24.5% for the carbonate ion concentrations of 0, 2, 5, 65, 150, and 250 mg/L, respectively. The results show that the removal efficiency of copper is not affected by the presence of carbonate below 5 mg/L. A significant reduction in removal efficiency was observed (more than 5 mg/L of carbonate concentration) caused by the passivation of anode, resulting in the hindering of the dissolution process of anode.

Phosphate. The concentration of phosphate ion was increased from 0 to 50 mg/L at the contaminant range of phosphate in the groundwater. The removal efficiency for copper was 97.8, 96.9, 77.3, 55.1, and 50% for 0, 2, 5, 25, and 50 mg/L of phosphate ion, respectively. There is no change in removal efficiency of copper below 5 mg/L of phosphate in the water. At higher concentrations (at and above 5 mgL^{-1}) of phosphate, the removal efficiency of copper decreased to 50%. The decrease in removal efficiency is attributable to the preferential adsorption of phosphate rather than copper as the concentration of phosphate increase.

Silicate. The effect of silicate on the removal efficiency of copper was investigated. The respective efficiencies for 0, 5, 10, and 15 mg/L of silicate are 97.8, 65, 60.2, and 53%. Removal of copper decreased with increasing silicate concentrations from 0 to 15 mg/L because of the preferential adsorption of copper. In addition to preferential adsorption, silicate can interact with iron hydroxide to form soluble and highly dispersed colloids that are not removed by normal filtration.

Fluoride. Results of this study show that the efficiency decreased by 97.8, 88.1, 71.5, 52, and 26.7% by increasing the concentration of fluoride from 0, 0.2, 0.5, 2, and 5 mg/L, respectively. This is attributable to the preferential adsorption of fluoride over copper as the concentration of fluoride increases. As such, when fluoride ions are present in the water to be treated, fluoride ions compete greatly with copper ions for the binding sites.

Adsorption Kinetics. The dynamics of the adsorption process in terms of the order and the rate constant can be evaluated using kinetic adsorption data. The process of copper removal from an aqueous phase by any adsorbent can be explained by using kinetic models.

Table 1—Comparison between the experimental and calculated q_e values for different initial copper concentrations in first-order and second-order adsorption isotherms at room temperature.

Concentration mg/L	q_e (exp) (mg/g)	First-order kinetics			Second-order kinetics		
		q_e (cal) (mg/g)	K_1 (min/mg)	R^2	q_e (cal) (mg/g)	K_2 (min/mg)	R^2
2	1.81	0.7133	−0.0256	0.9451	1.551	0.4091	0.9997
4	3.25	1.5542	−0.0221	0.9325	3.219	0.3221	0.9998
6	5.03	2.3124	−0.0136	0.9455	4.991	0.2454	0.9998
8	7.16	3.2245	−0.0102	0.812	7.018	0.1936	0.9842
10	8.65	5.0645	−0.0096	0.9014	8.559	0.0881	0.9999

Table 2—Elovich model and intraparticle diffusion for different initial copper concentrations at temperature 305 K and pH 7.

	Elovich model			Intraparticle diffusion		
Concentration mg L^{-1}	A (mg/g·h)	B (g/mg)	R^2	k_{id} (L/h)	A (%/h)	R^2
2	8.21	43.21	0.7878	20.21	0.145	0.8017
4	5.99	34.53	0.8431	15.44	0.101	0.6124
6	2.64	17.27	0.7036	13.07	0.099	0.7475
8	1.12	15.47	0.8213	12.88	0.087	0.8344
10	0.99	10.12	0.6374	10.14	0.056	0.5145

First- and Second-Order Rate Equation. The variation of the adsorbed copper with time was kinetically characterized using the first- and second-order rate equation proposed by Lagergren. The first-order Lagergren model is as follows (Ho et al., 1998; Wan Ngah et al., 2008):

$$dq/dt = k_1(q_e - q_t) \quad (4)$$

Where

q_t = the amount of copper adsorbed on the adsorbent at time t (min) and
k_1 (1/min) = the rate constant of first-order adsorption.

The integrated form of the aforementioned equation with the boundary conditions t = 0 to >0 (q = 0 to >0) can be rearranged to obtain the following time-dependence function:

$$\log(q_e - q_t) = \log(q_e) - k_1 t/2.303 \quad (5)$$

where q_e is the amount of copper adsorbed at equilibrium. The q_e and rate constant k_1 were calculated from the slope of the plots of log $(q_e - q_t)$ vs time (t).

The second-order kinetic model is expressed as (Benaissa and Elouchd, 2007; Wu et al., 2005)

$$dq/dt = k_2(q_e - q_t)^2 \quad (6)$$

Equation 6 can be rearranged and linearized as

$$t/q_t = 1/k_2 q_e^{\,2} + t/q_e \quad (7)$$

Where

q_e and q_t = the amount of copper adsorbed on $Fe(OH)_2$ (mg/g) at equilibrium and at time t (min), respectively, and
k_2 = the rate constant for the second-order kinetic model.

The equilibrium adsorption capacity, q_e(cal) and k_2, were determined from the slope and intercept of plot of t/q_t vs t (see Figure 3). The plots were found to be linear with good correlation coefficients (0.9997, 0.9998, 0.9998, 0.9842, and 0.9999 for 2, 4, 6, 8, and 10 mg/L initial copper concentration, respectively) and the theoretical q_e(cal) values agree well with the experimental q_e(exp) values at all concentrations studied. This implies that the second-order model is in good agreement with experimental data and can be used to favorably explain the copper adsorption on $Fe(OH)_2$.

Elovich Model and Intraparticle Diffusion. The simplified form of the Elovich model is (Oke et al., 2008)

$$q_t = 1/\beta \log_e(\alpha\,\beta) + 1/\beta \log_e(t) \quad (8)$$

Where

α = the initial adsorption rate (mg $g^{-1}.h^{-1}$) and
β = the desorption constant (g mg^{-1}).

If copper adsorption fits the Elovich model, a plot of q_t vs $\log_e(t)$ should yield a linear relationship with the slope of $(1/\beta)$ and an intercept of $1/\beta \log_e(\alpha\,\beta)$. Table 2 shows the results obtained from the Elovich equation. The lower regression value shows the inapplicability of this model.

Intraparticle diffusion is expressed as (Allen et al., 1989; Weber and Morris, 1963)

$$R = k_{id}(t)^a \quad (9)$$

A linearized form of eq 9 is followed by

$$\log R = \log k_{id} + a \log(t) \quad (10)$$

in which "a" depicts the adsorption mechanism and k_{id} may be taken as the rate factor (percent of copper adsorbed per unit time). Lower and higher values of k_{id} illustrate an enhancement in the rate of adsorption and better adsorption with improved bonding.

Table 1 and Table 2 depict the computed results obtained from first-order, second-order, Elovich, and intraparticle diffusion models. The correlation coefficient values decrease from second-order to first-order and from intraparticle diffusion to Elovich models. This indicates that the adsorption follows second order more than the other models. Furthermore, the calculated q_e values agree well with the experimental q_e values

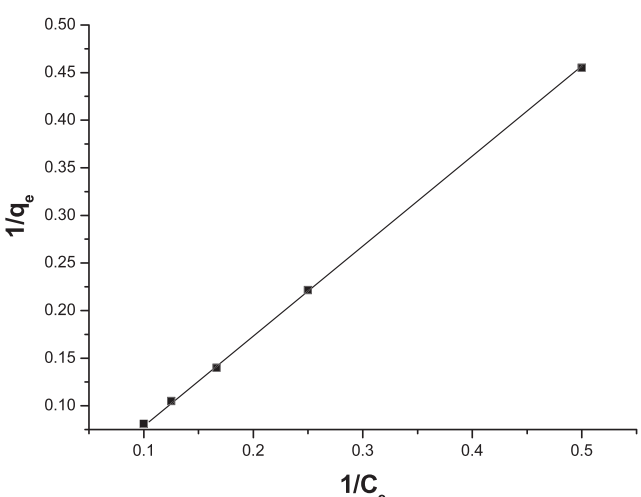

Figure 4—Langmuir plot for the adsorption of copper at pH 7.0, a current density of 0.02 A/dm^2, and a temperature of 303 K.

Table 3—Constant parameters and correlation coefficient calculated for different adsorption isotherm models at different temperatures for copper adsorption on iron hydroxide.

Isotherm	Constants			
Langmuir	q_m (mg/g)	b (L/mg)	R_L	R^2
	219.36	0.498	0.9325	0.9999
Freundlich	K_f (mg/g)	n (L/mg)		R^2
	0.9545	1.665		0.9665
D–R	q_s ($\times 10^3$ mol/g)	B ($\times 10^3$ mol^2/kJ^2)	E (kJ/mol)	R^2
	1.312	2.112	11.25	0.9325

for the second-order kinetics model, concluding that the second-order kinetics equation is the best fitting kinetic model.

Adsorption Isotherm. The adsorption capacity of the adsorbent has been tested using Freundlich, Langmuir, and Dubinin–Redushkevich isotherms. These models have been widely used to describe the behavior of adsorbent-adsorbate couples. To determine the isotherms, the initial pH was kept at 7 and the concentration of copper used was in the range of 2 to 10 mg/L.

Freundlich Isotherm. The Freundlich isotherm is an empirical model relating to the adsorption intensity of the sorbent toward adsorbent. The isotherm is adopted to describe reversible adsorption and is not restricted to monolayer formation. The mathematical expression of the Freundlich model can be written as (Larous et al., 2005; Lee et al., 2004; Prasanna Kumar et al., 2005)

$$q_e = KC_e^{\,n} \tag{11}$$

According to the Freundlich isotherm model, initially amount of adsorbed compounds increases rapidly; this increase slows down with increasing surface coverage. Equation 11 can be linearized in logarithmic form and the Freundlich constants can be determined as follows:

$$\log q_e = \log k_f + n \log C_e \tag{12}$$

Where

k_f = the Freundlich constant related to adsorption capacity,
n = the energy or intensity of adsorption, and
C_e = the equilibrium concentration of copper (mg/L).

Table 4—Pore diffusion coefficients for the adsorption of copper at various concentrations and temperatures.

Concentration (mg/L)	Pore diffusion constant D × 10^{-9} (cm^2/s)
2	1.221
4	1.016
6	0.942
8	0.778
10	0.721

Temperature (K)	Pore diffusion constant D × 10^{-9} (cm^2/s)
313	1.545
323	1.153
333	0.988
343	0.886

In testing the isotherm, the copper concentration used was 2 to 10 mg/L and, at an initial concentration of pH 7, the adsorption data are plotted as logq_e vs logC_e and should result in a straight line with slope ''n'' and intercept K_f. The intercept and the slope are indicators of adsorption capacity and adsorption intensity, respectively. The value of ''n'' in the range of 1 to 10 indicates favorable sorption. The Freundlich constants k_f and ''n'' values are 0.9545 (mg/g) and 1.665 (L/mg), respectively. The results show that the Freundlich plots fit satisfactorily with the experimental data obtained in the present study.

Langmuir Isotherm. The linearized form of the Langmuir adsorption isotherm model is (Bouzid et al., 2008; Sarioglu et al., 2005)

$$C_e/q_e = 1/q_m b + C_e/q_m \tag{13}$$

Where

q_e = amount adsorbed at equilibrium concentration, C_e;
q_m = the Langmuir constant representing maximum monolayer adsorption capacity; and
b = the Langmuir constant related to the energy of adsorption.

The plots of $1/q_e$ as a function of $1/C_e$ for the adsorption of copper on $Fe(OH)_2$ are shown in Figure 4. The plots were found to be linear with good correlation coefficients (>0.99), indicating

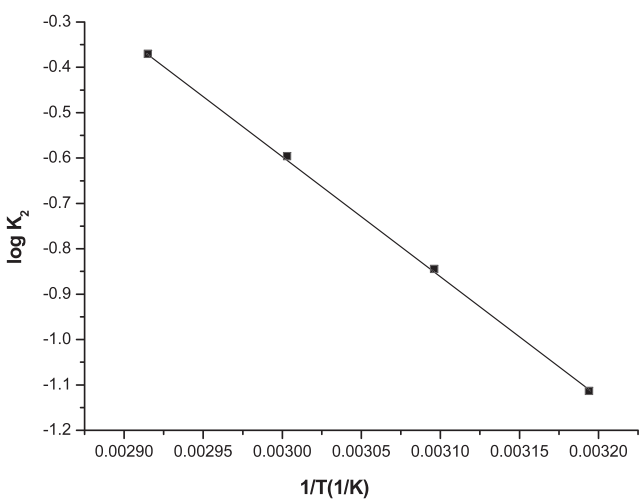

Figure 5—Plot of log k_2 and 1/T at pH 7.0 and a current density of 0.02A/dm^2 at various temperatures.

Table 5—Thermodynamic parameters for the adsorption of copper.

Temperature(K)	K_c	$\Delta G°$ (kJ/mol)	$\Delta H°$ (kJ/mol)	$\Delta S°$ (J/mol K)
313	0.2454	−706.12	20.331	2.994
323	0.5021	−1554.3		
333	0.7645	−2048.5		
343	1.1224	−2564.7		

the applicability of the Langmuir model in the present study. The values of monolayer capacity (q_m) were found to be 219.36 mg/g and the Langmuir constant (b) was found to be 0.498 L/mg. The values of q_m calculated by the Langmuir isotherm were all close to the experimental values at given experimental conditions. These facts suggest that copper is adsorbed in the form of monolayer coverage on the surface of the adsorbent.

The essential characteristics of the Langmuir isotherm can be expressed as the dimensionless constant R_L, as follows:

$$R_L = 1/(1 + bC_o) \quad (14)$$

Where

R_L = the equilibrium constant, which indicates the type of adsorption;
b = the Langmuir constant, and
C_o = various concentrations of copper solution.

The R_L values between 0 and 1 indicate favorable adsorption (Bouzid et al., 2008; Sarioglu et al., 2005). The R_L values were found to be between 0 and 1 for all the concentrations of copper studied.

Dubinin–Radushkevich Isotherm. Dubinin and Radushkevich proposed another isotherm that can be used to analyze equilibrium data. It is not based on the assumption of homogeneous surface or constant adsorption potential, but is applied to estimate the mean free energy of adsorption (E). This model is represented by (Tan et al., 2007)

$$q_e = q_s \exp(-B\varepsilon^2) \quad (15)$$

Where

ε = RT ln [1+1/C_e],
B = the free energy of sorption per mole of the adsorbate as it migrates to the surface of the electrocoagulant from infinite distance in the solution, and
q_s = the Dubinin–Radushkevich (D–R) isotherm constant related to the degree of adsorbate adsorption by the adsorbent surface.

The linearized form of eq 15 is as follows:

$$\ln q_e = \ln q_s - 2B\ RT\ \ln[1 + 1/C_e] \quad (16)$$

The isotherm constants of q_s and B are obtained from the intercept and slope of the plot of lnq_e vs ε^2, respectively (Demiral et al., 2008). The constant, B, gives the mean free energy, E, of adsorption per molecule of the adsorbate when it is transferred to the surface of the solid from infinity in the solution. The relationship is given as

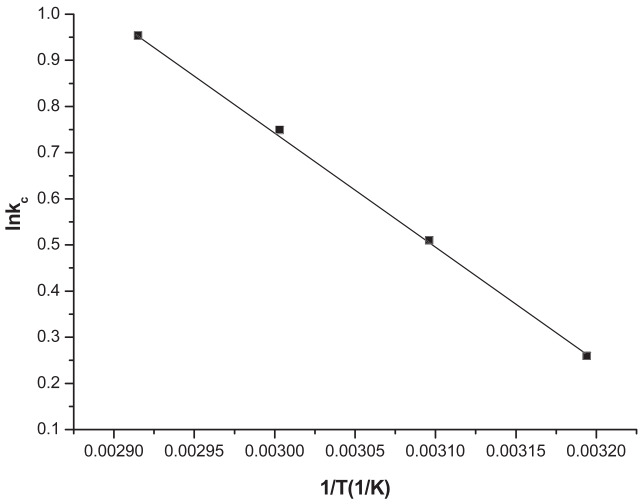

Figure 6—Plot of log k_c and 1/T at pH 7.0 and a current density of 0.02A/dm^2.

$$E = \left[1/\sqrt{2B}\right] \quad (17)$$

The magnitude of E is useful for estimating the type of adsorption process. It was found to be 11.25 kJ/mol, which is bigger than the energy range of the adsorption reaction, 8 to 16 kJ/mol (Oguz, 2005). As such, the type of adsorption of copper on iron hydroxide was defined as *chemical adsorption.*

The correlation coefficient values of different isotherm models are listed in Table 3. The Langmuir isotherm model has a higher regression coefficient ($R^2 = 0.999$) compared to the other models. The value of R_L for the Langmuir isotherm was calculated from 0 to 1, indicating the favorable adsorption of copper.

Effect of Temperature. The amount of copper adsorbed on the adsorbent increases by increasing the temperature, indicating that the process is endothermic. The diffusion coefficient, *D*, for intraparticle transport of copper species into the adsorbent particles was calculated at a different temperature by

$$t_{1/2} = 0.03 \times r_o^2/D \quad (18)$$

Where

$t_{1/2}$ = the time of half adsorption (s),
r_o = the radius of the adsorbent particle (cm), and
D = the diffusion coefficient in cm^2/s.

For all chemisorption systems, the diffusivity coefficient should be 10^{-5} to 10^{-13} cm^2/s (Yang and Al-Duri, 2001). In the present study, *D* is found to be in the range of 10^{-10} cm^2/s. The pore diffusion coefficient (*D*) values for various temperatures and different initial concentrations of copper are presented in Table 4.

To determine the energy of activation for adsorption of copper, the second-order rate constant is expressed in Arrhenius form (Golder et al., 2006) as follows:

$$\ln k_2 = \ln k_o - E/RT \quad (19)$$

Where

k_o = the constant of the equation (g/mg·min),
E = the energy of activation (J/mol),

Table 6—Comparison between the experimental and calculated q_e values for different initial copper concentrations of 10 mg L^{-1} in first- and second-order adsorption isotherm at various temperatures and at pH 7.

Temperature (K)	q_e (exp)	First-order adsorption			Second-order adsorption		
		q_e(Cal)	K_1 (min/mg)	R^2	q_e(Cal)	K_2 (min/mg)	R^2
313	8.71	1.499	−0.0022	0.9781	8.662	0.0733	0.9982
323	8.84	1.894	−0.0015	0.6845	8.912	0.1885	0.9999
333	9.12	2.955	−0.0009	0.8246	9.025	0.2422	0.9974
343	9.05	3.756	−0.0005	0.7556	9.215	0.3327	0.9966

R = the gas constant (8.314 J/mol/K), and
T = the temperature in K.

Figure 5 shows that the rate constants vary with temperature according to eq 19. The activation energy (0.545 kJ/mol) is calculated from the slope of the fitted equation. The free energy change is obtained using the following relationship:

$$\Delta G = -RT \ln K_c \quad (20)$$

Where

ΔG = the free energy (kJ/mol),
K_c = the equilibrium constant,
R = the gas constant, and
T = the temperature in K.

The Kc and ΔG values are presented in Table 5. The Kc values were calculated from activation energy. Table 5 shows that the negative value of ΔG indicates the spontaneous nature of adsorption. Other thermodynamic parameters such as entropy change (ΔS) and enthalpy change (ΔH) were determined using the van't Hoff equation as follows:

$$lnK_c = \frac{\Delta S}{R} - \frac{\Delta H}{RT} \quad (21)$$

The enthalpy change (ΔH = 20.331 kJ/mol) and entropy change (ΔS = 2.995 kJ/mol) were obtained from the slope and intercept of the van't Hoff linear plots of lnKc vs 1/T (see Figure 6). A positive value of enthalpy change (ΔH) indicates that the adsorption process is endothermic in nature, and the negative value of change in internal energy (ΔG) shows the spontaneous adsorption of copper on the adsorbent. Positive values of entropy change show the increased randomness of the solution interface during the adsorption of copper on the adsorbent (see Table 5). Enhancement of the adsorption capacity of electrocoagulant (iron hydroxide) at higher temperatures may be attributed to the enlargement of pore size and/or activation of the adsorbent surface. Using the Lagergren rate equation, first-order rate constants and correlation coefficients were calculated for different temperatures (305 to 343 K). The calculated "q_e" values obtained from second-order kinetics agree with the experimental "q_e" values better than the first- order kinetics model. Table 6 depicts the computed results obtained of second-order kinetics models. These results indicate that the adsorption follows the second-order kinetic model at different temperatures used in this study.

Process Scale-Up Studies. The results showed that the maximum removal efficiency of 97.8% was achieved at a current density of 0.02 A/dm^2 and a pH of 7 using mild steel as anode and stainless steel cathode. The results were consistent with laboratory-scale results, showing that the process was technologically feasible.

Sludge Characterization

Scanning Electron Microscope and Energy-Dispersive X-Ray Spectroscopy Studies. Figure 7 shows the SEM image of the mild steel anode after several cycles of use in electrocoagulation experiments in copper electrolyte. The electrode surface is found to be rough, with a number of dents. These dents are formed around the nucleus of the active sites where the electrode dissolution results in the production of iron hydroxides. The formation of a large number of dents may be attributed to the anode material consumption at active sites because of the generation of oxygen at its surface of electrode.

Energy-dispersive analysis of X-rays was used to analyze the elemental constituents of copper-adsorbed iron hydroxide shown in Figure 8. It shows that the presence of Cu, Mg, and O appears in the spectrum. Energy-dispersive X-ray spectroscopy analysis provides direct evidence that copper is adsorbed on iron hydroxide.

Fourier Transform Infrared Studies. Figure 9 presents the FTIR spectrum of copper-iron hydroxide. A broad adsorption band at 3452.84 cm^{-1} implies the transformation from free protons into a proton-conductive state in brucite. The 1628.43-cm^{-1} peak indicates the bent vibration of H-O-H. Absorbance at 1387.88 cm^{-1}, which could be assigned to the binding of copper to the carboxyl group and the band at 629.93 cm^{-1}, corresponds to the Fe-O stretching vibration.

Conclusions

The results showed that the optimized removal efficiency of 97.8% was achieved at a current density of 0.02A/dm^2 and a pH of 7.0 using mild steel and stainless steel as anode and cathode. The iron hydroxide generated in the cell removes the copper present in the water and reduces the copper concentration to less than 1 mg/L, making it suitable for drinking. The results show that the process was technologically feasible. The Langmuir adsorption isotherm was found to fit the equilibrium data for copper adsorption. The adsorption process follows second-order kinetics. Temperature studies showed that adsorption was endothermic and spontaneous in nature.

Acknowledgments

The authors wish to express their gratitude to the director of the Central Electrochemical Research Institute, Karaikudi, for aid in publishing this article.

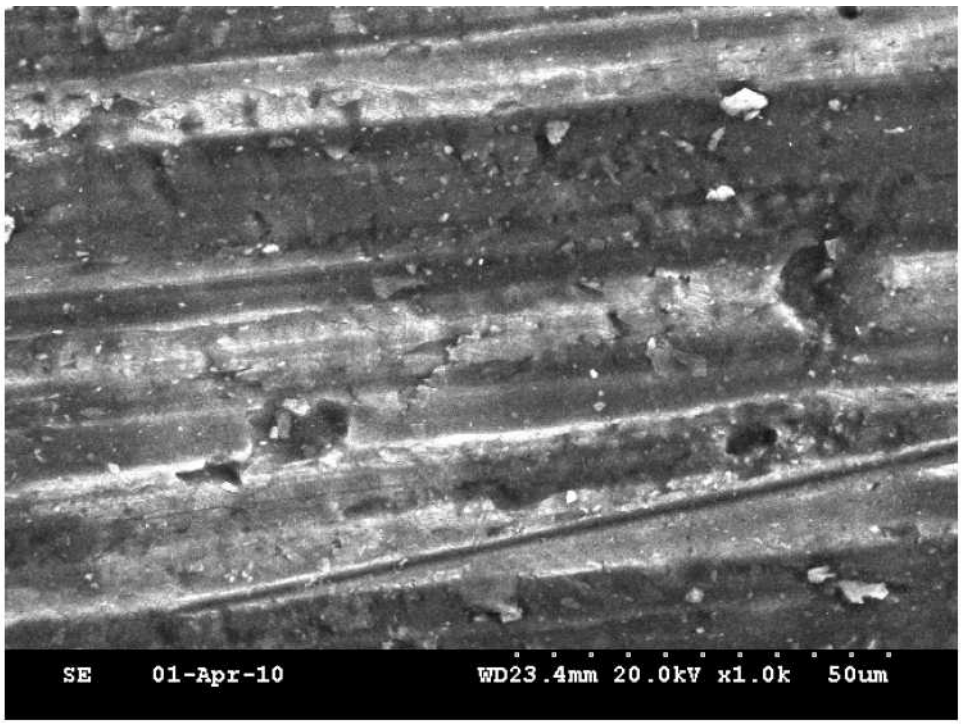

(a)

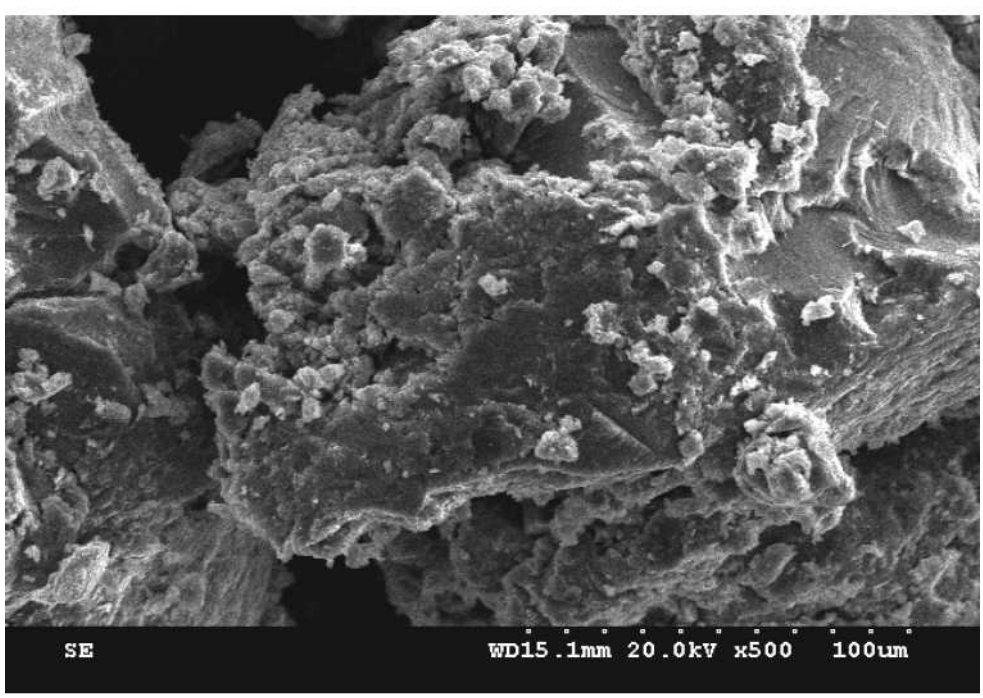

(b)

Figure 7—Scanning electron microscope image of the anode (a) before and (b) after treatment.

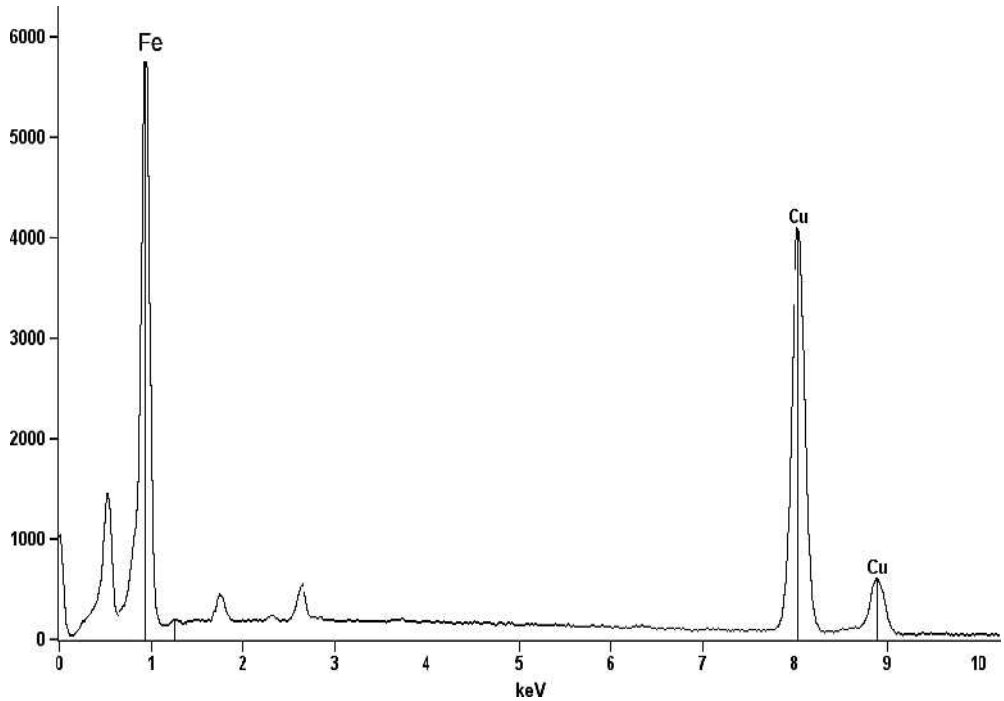

Figure 8—Energy-dispersive X-ray spectroscopy for copper-adsorbed electrocoagulant.

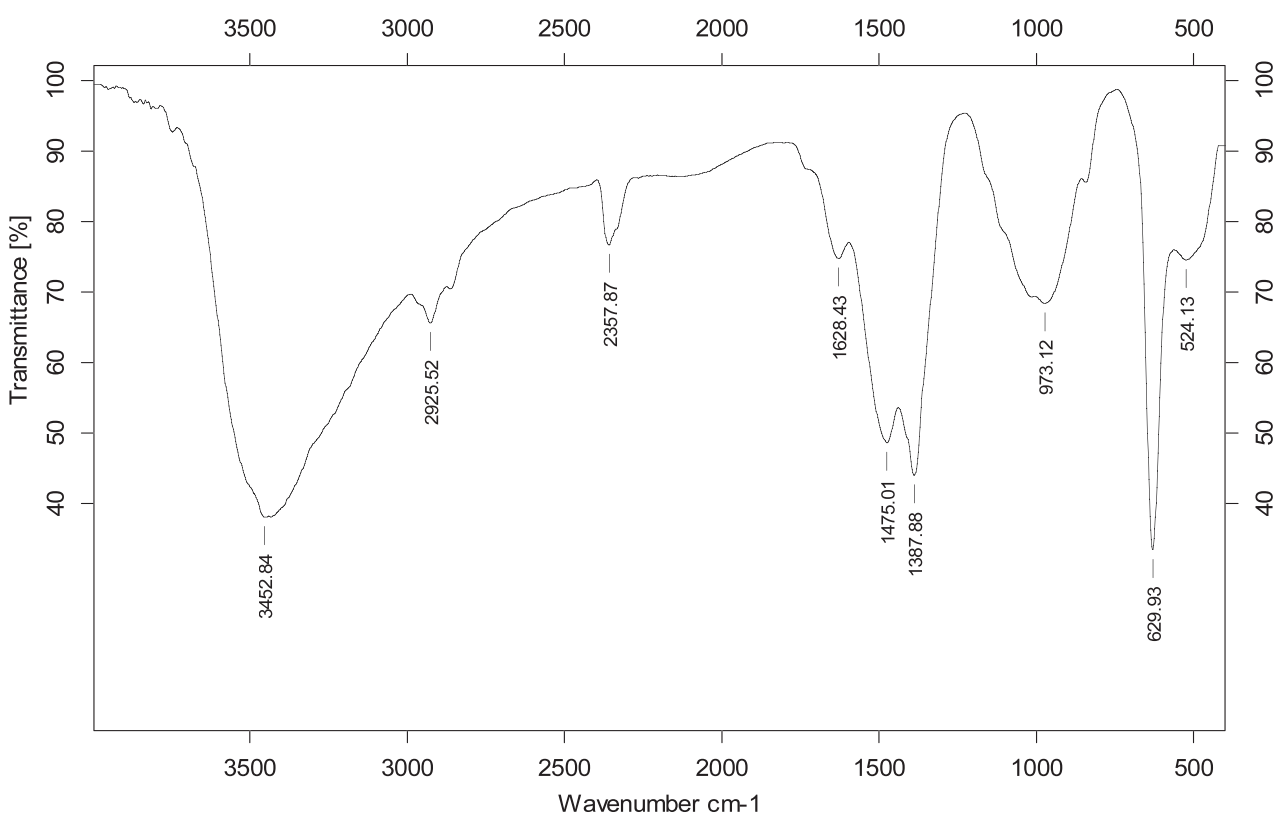

Figure 9—Fourier transform infrared spectrum for copper-adsorbed electrocoagulant.

Submitted for publication January 4, 2011; revised manuscript submitted May 5, 2011; accepted for publication June 16, 2011.

References

Adhoum, N.; Monser, L. (2004) Decolourization and Removal of Phenolic Compounds from Olive Mill Wastewater by Electrocoagulation. *Chem. Eng. Process.*, **43,** 1281–1287.

Ajmal, M.; Khan, A.; Ahmad, S.; Ahmad, A. (1998) Role of Sawdust in the Removal of Copper(II) from Industrial Wastes. *Water Res.*, **32,** 3085–3091.

Allen, S. J.; Mckay, G.; Khader K. H. Y. (1989) Intraparticle Diffusion of Basic Dye during Adsorption onto Sphagnum Peat. *Environ. Pollut.*, **56,** 39–50.

Bailey, S. E.; Olin, T. J., Bricka, R. M., Adrian, D. D. (1999) A Review of Potentially Low-Cost Sorbents for Heavy Metals. *Water Res.*, **33,** 2469–79.

Benaissa, H.; Elouchd, M. A. (2007) Removal of Copper Ions from Aqueous Solutions by Dried Sunflower Leaves. *Chem. Eng. Process.*, **46,** 614–622.

Billon, L.; Meric, V.; Castetbon, A.; Francois, J.; Desbrieres, J. (2006) Removal of Copper Ions from Water of Boilers by a Modified Natural Based Corncobs L. *J. Appl. Polym. Sci.* **102,** 4637–4645.

Boujelben, N.; Bouzid, J.; Elouear, Z. (2009) Adsorption of Nickel and Copper onto Natural Iron Oxide-Coated Sand from Aqueous Solutions: Study in Single and Binary Systems. *J. Hazard. Mater.*, **163,** 376–382.

Bouzid, J.; Elouear, Z.; Ksibi, M.; Feki, M.; Montiel, A. (2008) A Study on Removal Characteristics of Copper from Aqueous Solution by Sewage Sludge and Pomace Ashes. *J. Hazard. Mater.*, **152,** 838–845.

Carlesi Jara, D.; Fino, V.; Specchia, G.; Saracco, P. (2007) Electrochemical Removal of Antibiotics from Wastewaters. *Appl. Catals B: Environ.*, **70,** 479–487.

Carlos, A.; Huitle, M.; Ferro, S. (2006) Electrochemical Oxidation of Organic Pollutants for Wastewater Treatment: Direct and Indirect Processes. *Chem. Soc. Rev.* **35,** 1324–1340.

Chen, G. (2004) Electrochemical Technologies in Wastewater Treatment. *Sep. Purif. Technol.*, **38,** 11–41.

Christensen, P. A.; Egerton, T. A.; Lin, W. F.; Meynet, P.; Shaoa, Z. G.; Wright, N. G. (2006) A Novel Electrochemical Device for the Disinfection of Fluids by OH Radicals. *Chem. Commun.*, **38,** 4022–4023.

Central Pollution Control Board, Ministry of Environment and Forests, Government of India, Delhi. http://www.cpcb.nic.in (accessed Feb 2012).

Demiral, H.; Demiral, I.; Tumsek, F.; Karacbacakoglu, B. (2008) Adsorption of Chromium (Vl) from Aqueous Solution by Activated Solution by Activated Carbon Derived from Olive Bagasse and Applicability of Different Adsorption Models. *Chem. Eng. J.*, **144,** 188–195.

Fiol, N.; Villaescesa, I.; Martınez, M.; Miralles, N.; Poch, J.; Serarols, J. (2006) Sorption of Pb(II), Ni(II), Cu(II) and Cd(II) from Aqueous Solutions by Olive Stone Waste. *Sep. Purif. Technol.*, **50,** 132–140.

Gardea-Torresdey, J. L.; Tang, L.; Salvador, J. M. (1996) Copper Adsorption by Esterified and Unesterified Fractions of Sphagnum Peat Moss and its Different Humic Substances. *J. Hazard. Mater.*, **48,** 191–206.

Golder, A. K.; Samantha, A. N.; Ray, S. (2006) Removal of Phosphate from Aqueous Solution using Calcined Metal Hydroxides Sludge Waste Generated from Electrocoagulation. *Sep. Purif. Technol.*, **52,** 102–109.

Ho, Y. S.; McKay, G. (1998) A Comparison of Chemisorption Kinetic Models Applied to Pollutant Removal on Various Sorbents. *Process Safety Environ. Protection*, **76,** 332–340.

James, R.; Sampath, K.; Selvamani, P. (2006) Effect of Ion-Exchanging Agent, Zeolite on Removal of Copper in Water and improvement of Growth in Oreochromis mossambicus (Peters). *Asian Fisheries Sci.*, **13,** 317–325.

Larous, S.; Meniai, H.; Bencheikh Lehocine, M. (2005) Experimental Study of the Removal of Copper from Aqueous Solutions by Adsorption using Sawdust. *Desalination*, **185,** 483–490.

Lee, C.-I.; Yanga, W.; Hsiehb, C.-I. (2004) Removal of Copper (II) by Manganese-Coated Sand in a Liquid Fluidized-Bed Reactor. *J. Hazard. Mater.*, **B114,** 45–51.

Miwa, D. W.; Malpass, G. R. P.; Machado, S. A. S.; Motheo, A. J. (2006) Electrochemical Degradation of Carbaryl on Oxide Electrodes. *Water Res.*, **40,** 281–289.

Mrozowski, J.; Zielinski, J. (1983) Studies of Zinc and Lead Removal from Industrial Wastes by Electrocoagulation. *Environ. Protection Eng.*, **9,** 77–85.

Oguz, E.; (2005) Adsorption Characteristics and the Kinetics of the Cr(VI) on the Thuja Oriantalis. *Colloid Surf. A.*, **252**, 121–128.

Oke, I. A.; Olarinoye, N. O.; Adewusi, S. R. A. (2008) Adsorption Kinetics for Arsenic Removal from Aqueous Solutions by Untreated Powdered Eggshell. *Adsorption*, **14,** 73–83.

Onder, E.; Koparal, A. S.; Ogutveren, U. B. (2007) An Alternative Method for the Removal of Surfactants from Water: Electrochemical Coagulation. *Sep. Purif. Technol.*, **52,** 527–532.

Onmez, G.; Aksu, Z. (1999) The Effect of Copper(II) Ions on the Growth and Bioaccumulation Properties of Some Yeasts. *Process Biochem.*, **35,** 35–142.

Ozcan, A.; Ozcan, A. S.; Tunali, S.; Akar, T.; Kiran, I. (2005) Determination of the Equilibrium, Kinetic and Thermodynamic Parameters of Adsorption of Copper (II) Ions onto Seeds of Capsicum Annuum. *J. Hazard. Mater.*, **B124,** 200–208.

Ozer, A.; Ozer, D.; Ozer, A. (2004) The Adsorption of Copper(II) Ions onto Dehydrated Wheat Bran (DWB): Determination of the Equilibrium and Thermodynamic Parameters. *Process Biochem.*, **39,** 2183–2191.

Papandreou, A.; Stournaras, C. J.; Panias, D. (2007) Copper and Cadmium Adsorption on Pellets Made from Fired Coal Fly Ash. *J. Hazard. Mater.*, **148,** 538–547.

Prasad, M. N. V.; Freitas, H. (2000) Removal of Toxic Metals from Solution by Leaf, Stem and Root Phytomass of Quercus Ilex L. (Holly Oak). *Environ. Pollut.*, **110,** 277–283.

Prasanna Kumar, Y.; King, P.; Prasad, V. S. R. K. (2006) Removal of Copper from Aqueous Solution using *Ulva Fasciata* sp.—A Marine Green Algae. *J. Hazard. Mater.*, **B137,** 367–373.

Saeed, A.; Iqbal, M.; Akhtar, M. W. (2005) Removal and Recovery of Lead(II) from Single and Multimetal (Cd, Cu, Ni, Zn) Solutions by Crop Milling Waste (Black Gram Husk). *J. Hazard. Mater.*, **B117,** 65–73.

Sarioglu, M.; May, A.; Cebeci, Y. (2005) Removal of Copper from Aqueous Solutions by Phosphate Rock. *Desalination*, **181,** 303–311.

Shukla, S. P.; Sakhardane, V. D. (1992) Column Studies on Metal Ion Removal by Dyed Cellulosic Materials. *J. Appl. Poly. Sci.*, **44,** 903–910.

Tan, I. A. W.; Hameed, B. H.; Ahmed, A. L. (2007) Equilibrium and Kinetics Studies on the Basic Dye Adsorption by Palm Fibre Activated Carbon. *Chem. Eng. J.*, **127,** 111–119.

Vasudevan, S.; Lakshmi, J.; Jayara, J.; Sozhan, G. (2009) Remediation of Phosphate-Contaminated Water by Electrocoagulation with Aluminum, Aluminum Alloy and Mild Steel Anodes. *J. Hazard. Mater.*, **164,** 1480–1486.

Vasudevan, S.; Lakshmi, J.; Vanathi, R. (2010) Electrochemical Coagulation for Chromium Removal: Process Optimization, Kinetics, Isotherm and Sludge Characterization. *Clean*, **38,** 9–16.

Villaescesa, I.; Fiol, N.; Martinez, M.; Miralles, N.; Poch, J.; Serarols, J. (2004) Removal of Copper and Nickel Ions from Aqueous Solutions by Grape Stalk Wastes. *Water Res.*, **38,** 992–1002.

Vinikour, W. S.; Goldstein, R. M.; Anderson, R. V. (1980) Bioaccumulation Patterns of Zinc, Copper, Cadmium and Lead in Selected Fish Species from the Fox River. *Illinois. Bull. Environ. Contam. Toxicol.*, **24,** 727–734.

Wan Ngah, W. S.; Hanafiah, M. A. K. M. (2008) Adsorption of copper on rubber (*Hevea brasiliensis*) Leaf Powder: Kinetic, Equilibrium and Thermodynamic Studies. *Biochem. Eng. J.*, **39,** 521–530.

Weber, W. J., Jr.; Morris, J. C. (1963) Kinetics of Adsorption on Carbon from Solutions. *J. Sanit. Eng. Div., Proc. Am. Soc. Civ. Eng.*, **89,** 31–59.

Wu, Z.; Joo, H.; Lee, K. (2005) Kinetics and Thermodynamics of the Organic Dye Adsorption on the Mesoporous Hybrid Xerogel. *Chem. Eng. J.*, **112,** 227–36.

Yang, X. Y.; Al-Duri, B. (2001) Application of Branched Pore Diffusion Model in the Adsorption of Reactive Dyes on Activated Carbon. *Chem. Eng. J.*, **83,** 15–23.

Yu, B.; Zhang, Y.; Shukla, A.; Shukla, S. S.; Dorris, K. L. (2000) The Removal of Heavy Metal from Aqueous Solutions by Sawdust Adsorption-Removal of Copper. *J. Hazard. Mater.*, **80,** 33–42.